

**STUDY ON THE WETTING PROPERTIES,  
INTERFACIAL REACTIONS AND MECHANICAL  
PROPERTIES OF Sn-Zn AND Sn-Zn-Bi SOLDERS  
ON COPPER METALLIZATION**

**RAMANI MAYAPPAN**

**UNIVERSITI SAINS MALAYSIA**

**2007**

**STUDY ON THE WETTING PROPERTIES, INTERFACIAL REACTIONS AND  
MECHANICAL PROPERTIES OF Sn-Zn AND Sn-Zn-Bi SOLDERS ON  
COPPER METALLIZATION**

by

**RAMANI MAYAPPAN**

**Thesis submitted in fulfilment of the  
requirements for the degree  
of Doctor of Philosophy**

**September 2007**

## **ACKNOWLEDGEMENTS**

It is a satisfaction to recognize the help of many people who assisted me throughout the course of this study and in preparing this thesis. Special thanks to Associate Professor Dr. Luay Bakir Hussain and Professor Dr. Zainal Arifin Ahmad for their supervision, guidance and comments that make this thesis possible. Many thanks to Dean, Prof. Madya Dr. Khairun Azizi and all lecturers from the School of Materials and Mineral Resources Engineering for their supports. I wish to acknowledge the assistance of laboratory technical staffs: Mr. Shahrul, Mr. Rashid, Mr. Mokhtar, Mr. Azam and Mr. Mohamed.

I wish to thank Universiti Teknologi Mara for giving me study leave and financial support, which prompted the presentation of this thesis possible.

Many thanks to AUN SEED NET Geran and Prof. Ariga for supplying materials to make the research possible.

I acknowledge the contributions of En. Badri and Dr. Sunara for their support and assistance.

I would like to acknowledge the contributions of my friends in helping and guiding me throughout my stay in Universiti Sains Malaysia.

My sincere appreciation to my beloved wife, Siamala, for her constant support and patience. Finally, I thank all my family members who direct or indirectly contributed for the presentation of this thesis possible.

Ramani Mayappan

# CONTENTS

	<b>PAGE</b>
ACKNOWLEDGEMENTS	ii
TABLE OF CONTENTS	iii
LIST OF TABLES	x
LIST OF FIGURES	xi
LIST OF PLATES	xix
LIST OF ABBREVIATION	xx
LIST OF APPENDICES	xxi
LIST OF PUBLICATIONS & SEMINARS	xxii
ABSTRAK	xxiv
ABSTRACT	xxvi
<b>CHAPTER 1: INTRODUCTION</b>	
1.1 Problem Statement	1
1.2 Lead-free Solder	3
1.3 Lead-free Solder used in this Study	4
1.4 Importance of Study	6
1.5 Objective of the Study	9
1.6 Structure of the Thesis	9
<b>CHAPTER 2: LITERATURE REVIEW</b>	
2.1 Soldering	10
2.2 Lead	10
2.3 Sn-Pb Solder and Electronics Industries	11
2.4 Pb-free Solders Requirements	11

2.5	The Development of Pb-free Solders	15
2.6	Phase Diagrams	16
2.6.1	Sn-Pb Phase Diagram	17
2.6.2	Sn-Zn Phase Diagram	17
2.6.3	Sn-Cu Phase Diagram	19
2.6.4	Cu-Zn Phase Diagram	20
2.6.5	Sn-Bi Phase Diagram	20
2.6.6	Bi-Zn Phase Diagram	21
2.6.7	Cu-Pb Phase Diagram	21
2.6.8	Bi-Cu Phase Diagram	23
2.7	Copper as Interconnect Material	23
2.8	Solder Density	25
2.9	Flux in Soldering	25
2.10	Reflow Soldering	27
2.11	Wave Soldering	27
2.12	Solder Joint Reliability	27
2.13	Wetting Behavior of Molten Solders	28
2.14	Solder Wetting Measurements	30
2.14.1	Spreading Area Method	30
2.14.2	Wetting Balance Method	34
2.15	Surface Tension of the Molten Solder	40
2.16	Mechanical Properties of Solder Joints	42
2.16.1	Tensile Loading of Cu/Solder/Cu Joint	42
2.16.2	Shear Loading of Cu/Solder/Cu Joint	43
2.16.3	Shear Strength and Aging	45
2.17	Intermetallic Formation	46
2.17.1	Cu-Sn Intermetallic	48

2.17.2	Cu-Zn Intermetallic	50
2.18	Intermetallic Growth Kinetics	50
2.18.1	$\text{Cu}_5\text{Zn}_8$ Intermetallic Growth Kinetics	52
2.18.2	Intermetallic Growth of Other Lead-free Solders	53
<b>CHAPTER 3: MATERIALS, EQUIPMENTS AND EXPERIMENTAL PROCEDURES</b>		
3.1	Characterizations of the Raw Materials and Solders	54
3.1.1	Raw Materials used in the Study	54
3.1.1.1	Tin (Sn)	54
3.1.1.2	Zinc (Zn)	55
3.1.1.3	Copper (Cu) Substrates	56
3.1.2	Solder Preparations and Characterizations	56
3.1.2.1	Sn-40Pb Solder	56
3.1.2.2	Sn-9Zn Solder	57
3.1.2.3	Sn-8Zn-3Bi Solder	57
3.1.2.4	Elemental Analysis of Solders	57
3.1.3	Density Measurements of the Solders	58
3.1.4	Melting Temperature Measurements of the Solders using DSC	58
3.1.5	Microstructure Analysis of the Solders	58
3.2	Study on the Wettability and Interaction of solders with Copper Substrate	59
3.2.1	Solder Wettability Evaluation using Spreading Method	60
3.2.1.1	Preparation of Solder Cylinder	60
3.2.1.2	Spreading Test	61
3.2.1.3	Solder Spreading Area Measurement	61
3.2.1.4	Solder Contact Angle Measurement	63

3.2.1.5	Intermetallic Thickness Measurement	64
3.2.2	Wettability Evaluation using Dipping Method	65
3.2.2.1	Study of Effect of Solder Temperature and Flux on Wetting Properties	65
3.2.2.2	Surface Tension Calculation using Sample Perimeter (Circumference) Method	66
3.2.2.3	The Effect of Temperature on Intermetallic Formation	67
3.3	Mechanical Properties of Solder Joints	67
3.3.1	Reflow Temperature Profile	68
3.3.2	Mechanical Test using Butt Joint	68
3.3.2.1	Intermetallic Formation between Solder/Cu Interface	69
3.3.2.2	Tensile Test of the Butt Joint	70
3.3.2.3	Fracture Surface	70
3.3.3	Single Lap Shear Joint Test	70
3.3.3.1	Thermal Aging of the Solder Joints	72
3.3.3.2	Interface Phase Transformation of Cu/Solder/Cu Joints	72
3.3.3.3	Intermetallic Thickness Measurement of the Aged Samples	73
3.3.3.4	Tensile Shear Test of Aged Samples	73
3.4	Intermetallic Growth and Activation Energy Measurement of Cu/Solder/Cu Joints	74

## **CHAPTER 4: RESULTS AND DISCUSSION**

4.1	Characterization of the Raw Materials and Solders	75
-----	---	----

4.1.1	XRF Analysis of the Raw Materials	75
4.1.2	XRF Results of the Sn-40Pb, Sn-9Zn and Sn-8Zn-3Bi Solders	75
4.1.3	Density Results of the Sn-40Pb, Sn-9Zn and Sn-8Zn-3Bi Solders	76
4.1.4	Melting Temperature Results of the Sn-40Pb, Sn-9Zn and Sn-8Zn-3Bi Solders	77
4.1.5	Microstructure Analysis of the Bulk Solders	78
4.1.5.1	Optical Microscope Analysis of the Sn-40Pb, Sn-9Zn and Sn-8Zn-3Bi Solders	78
4.1.5.2	FEVPSEM Analysis of the Sn-40Pb, Sn-9Zn and Sn-8Zn-3Bi Solders Microstructure	78
4.2	Solder Wettability and Intermetallic Formation Results	81
4.2.1	Results of Solder Spreading on Copper Substrate	82
4.2.1.1	Spreading Area of the Sn-40Pb, Sn-9Zn and Sn-8Zn-3Bi Solders on Copper Substrate	82
4.2.1.2	Contact Angle of the Sn-40Pb, Sn-9Zn and Sn-8Zn-3Bi Solders on Copper Substrate	83
4.2.1.3	Intermetallic Formation Results Between Sn-40Pb, Sn-9Zn and Sn-8Zn-3Bi Solders and Cu Substrate using Spreading Method	88
4.2.1.4	Intermetallic Thickness Measurements of the Sn-40Pb/Cu, Sn-9Zn/Cu and Sn-8Zn-3Bi/Cu Joints	94
4.2.2	Results of Wettability using Dipping Method	96
4.2.2.1	The Effect of Temperature and Flux on Wetting Time	96



4.2.2.2	The Effect of Temperature and Flux on Maximum Wetting Force	99
4.2.2.3	The Effect of Temperature and Flux on Withdrawal Force	102
4.2.2.4	The Effect of Temperature and Flux on Contact Angle	104
4.2.2.5	Results of Surface Tension using Wetting Balance Method	106
4.2.2.6	Results on Intermetallic Formation between Sn-40Pb, Sn-9Zn and Sn-8Zn-3Bi Solders and Copper Substrate using Dipping Method	110
4.3	Results of Mechanical Properties of Solder Joints	112
4.3.1	Results of Tensile Butt Joint Test of Solder Joints	112
4.3.1.1	Interface Microstructure	113
4.3.1.2	Influence of Crosshead Speed on Solder Joint Strength	113
4.3.1.3	Fracture Morphologies and Failure Path in Butt-Joint Test	116
4.3.2	Results of Phase Transformation and Shear Test on Solder Joints after Solid-State Aging	118
4.3.2.1	Intermetallic Phase Transformation Results between Sn-40Pb/Cu Interface after Solid-State Aging	118
4.3.2.2	Intermetallic Phase Transformation Results between Sn-9Zn/Cu and Sn-8Zn-3Bi/Cu Interfaces after Solid-State Aging	123

4.3.2.3	Results of Intermetallic Phase Thickness Measurement	133
4.3.2.4	Results of Shear Test on Solder Joint	138
4.4	Growth Kinetics and Activation Energy for Intermetallic Growth	149
4.4.1	Growth Kinetics of Intermetallic	150
4.4.1.1	Growth Behavior for Sn-40Pb/Cu System	151
4.4.1.2	Growth Behavior for Sn-9Zn/Cu and Sn-8Zn-3Bi/Cu Systems	152
4.4.2	Activation Energy of Intermetallic Growth	154
4.4.2.1	Activation Energy of intermetallic Growth for Sn-40Pb/Cu System	155
4.4.2.2	Activation Energy of IMC Growth for Sn-9Zn/Cu and Sn-8Zn-3Bi/Cu Systems	156
<b>CHAPTER 5: CONCLUSIONS AND FUTURE WORKS</b>		
5.1	Conclusions	159
5.2	Future Works	160
<b>REFERENCES</b>		162
<b>APPENDICES</b>		

## LIST OF TABLES

	<b>PAGE</b>
Table 2.1 Major uses of lead globally	11
Table 2.2 World reserves for raw metals	13
Table 2.3 Raw metal cost	14
Table 2.4 Solder alloys cost	14
Table 2.5 Proposed lead-free solder alloys with their melting temperature	16
Table 2.6 Solder alloys density	25
Table 2.7 Wetting angles of some lead-free solders on Cu substrate using spreading test	33
Table 2.8 Wetting time on bare Cu coupons using wetting balance	38
Table 2.9 Wetting force on bare Cu coupons using wetting balance	39
Table 2.10 Contact angle on bare Cu coupons using wetting balance	40
Table 2.11 Surface tension values for Sn-Pb and some lead-free solder alloys	41
Table 2.12 Room temperature physical properties of Cu-Sn IMC	49
Table 2.13 Room temperature physical properties of Cu, Sn and Zn metals	49
Table 3.1 Flux used in the study	60
Table 4.1 Elemental compositions of raw materials	76
Table 4.2 Elemental compositions of solders	76
Table 4.3 Density of the bulk solders	76
Table 4.4 Differential scanning calorimetry analysis results of the solders	78
Table 4.5 Surface tension of the molten solders at 250°C	109
Table 4.6 Diffusion coefficient of Cu and Zn in Sn and Sn in Cu	125
Table 4.7 Literature value for $\gamma$ -Cu <sub>5</sub> Zn <sub>8</sub> phase growth rate constant	154
Table 4.8 The activation energy (Q) for the growth of $\gamma$ -Cu <sub>5</sub> Zn <sub>8</sub> intermetallic	158

## LIST OF FIGURES

	<b>PAGE</b>
Fig. 2.1 Sn-Pb binary phase diagram	18
Fig. 2.2 Sn-Zn binary phase diagram	18
Fig. 2.3 Cu-Sn binary phase diagram	19
Fig. 2.4 Cu-Zn binary phase diagram	20
Fig. 2.5 Sn-Bi binary phase diagram	21
Fig. 2.6 Bi-Zn binary phase diagram	22
Fig. 2.7 Cu-Pb binary phase diagram	22
Fig. 2.8 Bi-Cu binary phase diagram	23
Fig. 2.9 Cross section of the package: (a) Level 1 and Level 2 interconnection (b) A schematic illustration of Cu position in interconnection	24
Fig. 2.10 Schematic of thermodynamic equilibrium in wetting	31
Fig. 2.11 A typical sketch of wetting curve with the various moments of dipping experiment corresponds to the points of the wetting curve	35
Fig. 2.12 A typical non-wetting curve	36
Fig. 2.13 Sample coupon geometry for wetting balance test on molten solder alloy	37
Fig. 2.14 Solder bumps (joints) subjected to tensile loading due to substrate flexing (bending) during handling of the assembly	43
Fig. 2.15 Solder joints subjected to shear strain during thermal cycling due to CTE mismatch between the die, the solder and the substrate	44
Fig. 2.16 Relation between aging times and shear strength	45
Fig. 2.17 Crystal structure of the (a) $\eta$ -Cu <sub>6</sub> Sn <sub>5</sub> phase, (b) $\epsilon$ -Cu <sub>3</sub> Sn phase	48
Fig. 3.1 Research outline: characterization, wetting and mechanical testing	55

Fig. 3.2	Dialog box for setting scale	63
Fig. 3.3	Contact angle measurement	64
Fig. 3.4	Temperature profiles on the hotplate and aluminium plate	68
Fig. 3.5	Schematic diagram of the shear joint set up	71
Fig. 3.6	Single lap dog-bone shape (a) all dimensions in mm (b) Cu/solder/Cu joints	72
Fig. 4.1	Differential scanning calorimetry analysis profile of the solders	77
Fig. 4.2	Optical micrograph of (a) Sn-40Pb; (b) Sn-9Zn; and (c) Sn-8Zn- 3Bi	79
Fig. 4.3	FEVPSEM backscattered micrograph and EDX analysis of Sn- 40Pb solder	80
Fig. 4.4	FEVPSEM backscattered micrograph and EDX analysis of Sn- 9Zn solder	81
Fig. 4.5	FEVPSEM backscattered micrograph and EDX analysis of Sn- 8Zn-3Bi solder	82
Fig. 4.6	Solder spreading on Cu substrate for (a) Sn-40Pb, (b) Sn-9Zn and (c) Sn-8Zn-3Bi using ZnCl <sub>2</sub> flux at 280°C	83
Fig. 4.7	Spreading area on Cu substrate for Sn-40Pb, Sn-9Zn and Sn- 8Zn-3Bi solders at different temperatures using (a) HCl, (b) TB210, (c) MHS and (d) ZnCl <sub>2</sub> fluxes	84
Fig. 4.8	Contact angle on Cu substrate for Sn-40Pb, Sn-9Zn and Sn-8Zn- 3Bi solders at different temperatures using (a) HCl, (b) TB210, (c) MHS and (d) ZnCl <sub>2</sub> fluxes	84
Fig. 4.9	FEVPSEM backscattered images and EDX analysis of the Sn- 40Pb/Cu interface soldered using ZnCl <sub>2</sub> flux at (a) 220, (b) 250 and (c) 280°C	89

Fig. 4.10	FEVPSEM backscattered images of the Sn-9Zn/copper interface using HCl flux soldering at (a) 220 (b) 250 and (c) 280°C	91
Fig. 4.11	FEVPSEM backscattered images of the Sn-8Zn-3Bi/copper interface using ZnCl <sub>2</sub> flux soldering at (a) 220 (b) 250 and (c) 280°C	92
Fig. 4.12	IMC thickness of the solders using (a) HCl, (b) TB210, (c) MHS and (d) ZnCl <sub>2</sub> fluxes	95
Fig. 4.13	Wetting time (t <sub>0</sub> ) curve for Sn-8Zn-3Bi solder using ZnCl <sub>2</sub> flux	97
Fig. 4.14	Temperature and flux effect on wetting time using (a) HCl (b) TB210 (c) MHS and (d) ZnCl <sub>2</sub> fluxes	98
Fig. 4.15	An example of wetting curve for Sn-8Zn-3Bi solder using MHS flux and 20s dipping time	100
Fig. 4.16	Temperature and flux effect on maximum wetting force using (a) HCl (b) TB210 (c) MHS and (d) ZnCl <sub>2</sub> fluxes	101
Fig. 4.17	Schematic diagram of withdrawal process	103
Fig. 4.18	Temperature and flux effect on withdrawal force using (a) HCl (b) TB210 (c) MHS and (d) ZnCl <sub>2</sub> fluxes	103
Fig. 4.19	Temperature and flux effect on contact angle using (a) HCl (b) TB210 (c) MHS and (d) ZnCl <sub>2</sub> fluxes	105
Fig. 4.20	Substrate perimeter effect on maximum wetting force and withdrawal force for (a) Sn-40Pb, (b) Sn-9Zn and (c) Sn-8Zn-3Bi solders	108
Fig. 4.21	IMC formed with Cu and Sn-40Pb solder dipping for 20 s at (a) 220°C, (b) 250°C, (c) 280°C, (d) 300°C and (e) 330°C	110
Fig. 4.22	IMC formed with Cu and Sn-9Zn solder dipping for 20 s at (a) 220°C, (b) 250°C, (c) 280°C, (d) 300°C and (e) 330°C	111

Fig. 4.23	IMC formed with Cu and Sn-8Zn-3Bi solder dipping for 20 s at (a) 220°C, (b) 250°C, (c) 280°C, (d) 300°C and (e) 330°C	112
Fig. 4.24	The butt-joint as-soldered FEVPSEM backscattered microstructure image of the interface between (a) Sn-40Pb (b) Sn-9Zn and (c) Sn-8Zn-3Bi solders and Cu substrate	113
Fig. 4.25	Crosshead effects on solder joints strength	114
Fig. 4.26	Stress-strain curves of solder joints at room temperature for 0.2 mm/min crosshead speed	115
Fig. 4.27	FEVPSEM secondary electron image of fracture surface of the solder (a) Sn-40Pb, (b) Sn-9Zn and (c) Sn-8Zn-3Bi solders for 0.2 mm/min	116
Fig. 4.28	Solder joint break of (a) Sn-40Pb, (b) Sn-9Zn and (c) Sn-8Zn-3Bi solder for 0.2 mm/min	117
Fig. 4.29	Schematic picture showing failure at the solder/intermetallic boundary	117
Fig. 4.30	As-soldered IMC layer between Sn-40Pb and Cu substrate	118
Fig. 4.31	IMC layer formed between Sn-40Pb and Cu substrate isothermally aged at 50°C for 500h	119
Fig. 4.32	IMC layer formed between Sn-40Pb and Cu substrate isothermally aged at 75°C for (a) 100 hours and (b) 700 hours	119
Fig. 4.33	IMC layer formed between Sn-40Pb and Cu substrate isothermally aged at 150°C for 100h: (a) 300 X magnification, (b) 1000 X magnification and (c) EDX on Cu <sub>3</sub> Sn phase	120
Fig. 4.34	Transformation from scallop shape to planar layer as aging progresses: (a) 100°C for 250h (b) 125°C for 100h (c) 100°C for 500h (d) 125°C for 375h (e) 125°C for 700h and (f) 150°C for 375h	122

Fig. 4.35	IMC layer formed between Sn-40Pb and Cu substrate isothermally aged at 150°C for 700h	123
Fig. 4.36	IMC layer formed between solder/Cu joints for as-soldered for (a) Sn-9Zn and (b) Sn-9Zn-3Bi solders	124
Fig. 4.37	IMC layer formed between solder/Cu joints isothermally aged at 50°C for 700 hours for (a) Sn-9Zn and (b) Sn-8Zn-3Bi solders	124
Fig. 4.38	IMC layer formed between solder/Cu joints isothermally aged at 75°C for 100 hours for (a) Sn-9Zn (b) Sn-8Zn-3Bi solders	126
Fig. 4.39	IMC layer formed between solder/Cu joints isothermally aged at 75°C for 375 hours for (a) Sn-9Zn and (b) Sn-8Zn-3Bi solders	126
Fig. 4.40	IMC layer formed between solder/Cu joints isothermally aged at 100°C for 100 hours for (a) Sn-9Zn and (b) Sn-8Zn-3Bi solders	127
Fig. 4.41	IMC layer formed between solder/Cu joints isothermally aged at 125°C for 100 hours for (a) Sn-9Zn and (b) Sn-8Zn-3Bi solders	127
Fig. 4.42	IMC layer formed between solder/Cu joints isothermally aged at 125°C for 250 hours for (a) Sn-9Zn and (b) Sn-8Zn-3Bi solders	127
Fig. 4.43	IMC layer formed between solder/Cu joints isothermally aged at 125°C for 375 hours for (a) Sn-9Zn and (b) Sn-8Zn-3Bi solders	128
Fig. 4.44	IMC layer formed between solder/Cu joints isothermally aged at 125°C for 500 hours for (a) Sn-9Zn and (b) Sn-8Zn-3Bi solders	128
Fig. 4.45	IMC layer formed between solder/Cu joints isothermally aged at 125°C for 700 hours for (a) Sn-9Zn and (b) Sn-8Zn-3Bi solders	128
Fig. 4.46	IMC layer formed between solder/Cu joints isothermally aged at 150°C for 100 hours for Sn-9Zn solder	129
Fig. 4.47	IMC layer formed between solder/Cu joints isothermally aged at 150°C for 100 hours for Sn-8Zn-3Bi solder	130



Fig. 4.48	IMC layer formed between solder/Cu joints isothermally aged at 150°C for 250 hours for Sn-8Zn-3Bi solder	131
Fig. 4.49	IMC layer formed between solder/Cu joints isothermally aged at 150°C for 500 hours for Sn-8Zn-3Bi solder	131
Fig. 4.50	IMC layer formed between solder/Cu joints isothermally aged at 150°C for 700 hours for (a) Sn-9Zn and (b) Sn-8Zn-3Bi solders	132
Fig. 4.51	Schematic illustration of interfacial morphology change by heat exposure at 150°C at Sn-Zn/Cu interface	132
Fig. 4.52	Intermetallic thickness formed between Sn-40Pb, Sn-9Zn and Sn-8Zn-3Bi solders and Cu substrate aging at 50°C for 700 hours	134
Fig. 4.53	Intermetallic thickness formed between Sn-40Pb, Sn-9Zn and Sn-8Zn-3Bi solders and Cu substrate aging at 75°C for 700 hours	134
Fig. 4.54	Intermetallic thickness formed between Sn-40Pb, Sn-9Zn and Sn-8Zn-3Bi solders and Cu substrate aging at 100°C for 700 hours	134
Fig. 4.55	Intermetallic thickness formed between Sn-40Pb, Sn-9Zn and Sn-8Zn-3Bi solders and Cu substrate aging at 125°C for 700 hours	135
Fig. 4.56	Intermetallic thickness formed between Sn-40Pb, Sn-9Zn and Sn-8Zn-3Bi solders and Cu substrate aging at 150°C for 700 hours	135
Fig. 4.57	The effect of aging time on the strain at failure of Sn-40Pb, Sn-9Zn and Sn-8Zn-3Bi solder joints with Cu aged at (a) 50°C (b) 100°C and (c) 150°C	139
Fig. 4.58	The effect of aging time on the shear strength of Sn-40Pb, Sn-9Zn and Sn-8Zn-3Bi solder joints with Cu aged at (a) 50°C (b) 100°C and (c) 150°C	142
Fig. 4.59	FEVPSEM backscattered image of Sn-40Pb/Cu solder joint break: (a) at room temperature, (b) aged at 50°C for 500 hours, (c) aged at 100°C for 500 hours and (d) aged at 150°C for 500 hours	144

Fig. 4.60	FEVPSEM backscattered image of Sn-9Zn/Cu solder joint break: (a) at room temperature, (b) aged at 100°C for 500 hours and (c) aged at 150°C for 500 hours	145
Fig. 4.61	FEVPSEM backscattered image of Sn-8Zn-3Bi/Cu solder joint break: (a) at room temperature, (b) aged at 50°C for 100 hours, (c) aged at 100°C for 500 hours and (d) aged at 150°C for 250 hours	146
Fig. 4.62	FEVPSEM secondary electron micrographs of fracture surface of Sn-40Pb/Cu joint (a) Room temperature and aged (b) 100°C for 500 hours (c) 150°C for 500 hours	147
Fig. 4.63	FEVPSEM secondary electron micrographs of fracture surface of Sn-9Zn/Cu joint (a) Room temperature and aged (b) 100°C for 500 hours and (c) 150°C for 500 hours	148
Fig. 4.64	FEVPSEM secondary electron micrographs of fracture surface of Sn-8Zn-3Bi/Cu joint (a) Room temperature and aged (b) 100°C for 500 hours and (c) 150°C for 500 hours	149
Fig. 4.65	The relationship between IMCs thickness and aging time ( $t^{1/2}$ ) for Sn-40Pb/Cu system	152
Fig. 4.66	The relationship between IMCs thickness and aging time ( $t^{1/2}$ ) for Sn-9Zn/Cu system	153
Fig. 4.67	The relationship between IMCs thickness and aging time ( $t^{1/2}$ ) for Sn-8Zn-3Bi/Cu system	153
Fig. 4.68	Growth rate constant variations with aging temperature	154
Fig. 4.69	Arrhenius plot of the $\text{Cu}_6\text{Sn}_5$ intermetallic layer growth for Sn-40Pb/Cu system	155
Fig. 4.70	Arrhenius plot of the $\text{Cu}_5\text{Zn}_8$ intermetallic layer growth for Sn-9Zn/Cu system	157

Fig. 4.71 Arrhenius plot of the  $\text{Cu}_5\text{Zn}_8$  intermetallic layer growth for Sn-8Zn- 157  
3Bi/Cu system

## LIST OF PLATES

	<b>PAGE</b>	
Plate 3.1	Copper plates: (a) Copper type A with 0.4 mm thickness, (b) Copper type B with 1.5 mm thickness	56
Plate 3.2	Sn-40Pb solder bar	56
Plate 3.3	Preparation of Sn-9Zn solder alloy	57
Plate 3.4	Sn-8Zn-3Bi solder bar	57
Plate 3.5	A Micromeritics Accupyc-1330, gas pycnometer	58
Plate 3.6	Solder Checker model SAT-5100, Rhesca	59
Plate 3.7	Fluxes: (a) HCl based (b) TB210 (c) MHS (d) Zinc Chloride	60
Plate 3.8	Solder cylinder preparations: (a) Mould, (b) Solder disc and cylinder	61
Plate 3.9	The spreading test: (a) Copper substrate with solder disc above the solder bath; (b) Schematic diagram of the spread test and (c) solder spreading on Cu	62
Plate 3.10	Spreading of solder: (a) before and (b) after crop	63
Plate 3.11	Mounted solder cross section: (a) Sn-40Pb, (b) Sn-9Zn and (c) Sn-8Zn-3Bi	64
Plate 3.12	Solders used as solder bath: (a) Sn-40Pb, (b) Sn-9Zn and (c) Sn-8Zn-3Bi	65
Plate 3.13	Copper strip on balance arm prior to dipping test	66
Plate 3.14	Butt joint: (a) Schematic illustration of joint dimensions, (b) optical picture of the joints	69
Plate 3.15	Instron machine for tensile test	70
Plate 3.16	Optical picture of joint surface showing wetting and non-wetting areas	74

## LIST OF ABBREVIATION

EPA	Environmental Protection Agency
WEEE	Waste Electrical and Electronic Equipment
RoHS	Restriction of Hazardous Substances
EU	European Union
JEIDA	Japanese Electronic Industry Development Institute Association
JIEP	Japanese Institute of Electronic Packaging
NEMI	National Electronic Manufacturing Initiation
NCMS	National Centre for Manufacturing Sciences
IPC	Association Connecting Electronics Industries
D	Diffusivity
IMC	Intermetallic Compound
NIST	National Institute of Standards and Technology
PCB	Printed Circuit Board
BGA	Ball Grid Array
Ni-Cu-P	Nickel-Copper-Palladium
RE	Rare Earth Elements
RA	Rosin Activated
RMA	Rosin Mild Activated
OFHC	Oxygen-Free High Conductivity
FEVPSEM	Field Emission Variable Pressure Scanning Electron Microscope
CTE	Coefficient of Thermal Expansion
EDX	Energy Dispersive X-ray
OM	Optical Microscope
SMT	Surface Mount Technology
BSD	Backscattered Electron
XRD	X-ray Diffraction

## LIST OF APPENDICES

- Appendix A Summary of the WEEE/RoHS Directive
- Appendix B Dipping rate effect on (a) maximum wetting force, (b) withdrawal and (c) end force using HCl flux
- Appendix C Effect of substrate perimeter on wetting time and contact angle
- Appendix D Phase transformation of Sn-40Pb aging at 50, 75, 100, 125 and 150°C for 100, 250, 375, 500 and 700 hours
- Appendix E Phase transformation of Sn-40Pb aging at 50, 75, 100, 125 and 150°C for 100, 250, 375, 500 and 700 hours
- Appendix F Phase transformation of Sn-8Zn-3Bi aging at 50, 75, 100, 125 and 150°C for 100, 250, 375, 500 and 700 hours
- Appendix G The growth rate constant obtain at each aging temperature
- Appendix H Journal paper 1
- Appendix I Journal paper 2
- Appendix J Proceeding 1
- Appendix K Journal paper 3

## LIST OF PUBLICATIONS & SEMINARS

- 1.1 Ramani Mayappan, Ahmad Badri Ismail, Zainal Arifin Ahmad, Tadashi Ariga and Luay Bakir Hussain. (2006) Effect of sample perimeter and temperature on Sn-Zn based lead-free solders. *Materials Letters*. **60**: 2383-2389.
- 1.2 Ramani Mayappan, Ahmad Badri Ismail, Zainal Arifin Ahmad, Tadashi Ariga and Luay Bakir Hussain. (2007) The effect of crosshead speed on the joint strength between Sn-Zn-Bi lead-free solders and Cu substrate. *Journal of Alloys and Compounds*. **436**: 112-117.
- 1.3 R. Mayappan, A.B. Ismail, Z.A. Ahmad, L.B. Hussain and T. Ariga. (2005) A Study on Microstructure and Wetting Properties of Eutectic Sn-Pb, Sn-Zn and Sn-Zn-Bi Lead-Free Solders using Wetting Balance Instrument. *Malaysian Journal of Microscopy*. **1**: 100-105.
- 1.4 R. Mayappan, A.B. Ismail, Z.A. Ahmad, T. Ariga and L.B. Hussain. (2005) Joint Strength and Interfacial Microstructure between Sn-Pb, Sn-Zn and Sn-Zn-Bi Solders on Cu Substrate. *Malaysian Journal of Microscopy*. **2**: 7-14.
- 1.5 Ramani Mayappan, Ahmad Badri Ismail, Zainal Arifin Ahmad, Tadashi Ariga and Luay Bakir Hussain. (2004) A study on microstructure and wetting properties of eutectic Sn-Pb, Sn-Zn and Sn-Zn-Bi lead-free solders. *Proceeding of International Conference on X-ray and Related Techniques in Research and Industry*. 15-16<sup>th</sup> September 2004. Penang, Malaysia. P. 1-13.
- 1.6 Ramani Mayappan, Ahmad Badri Ismail, Zainal Arifin Ahmad, Luay Bakir Hussain and Tadashi Ariga. (2004) Correlation study between wetting properties and surface roughness and the influence of fluxes on Sn-Pb, Sn-Zn and Sn-Zn-Bi lead-free solders. *Proceeding of 2<sup>nd</sup> National Postgraduate Colloquium on Materials, Minerals Resources and Polymers 2004*. 7-8<sup>th</sup> October 2004. Penang, Malaysia. P. 13-19.
- 1.7 Ramani Mayappan, Ahmad Badri Ismail, Zainal Arifin Ahmad, and Luay Bakir Hussain. (2004) A study on microstructure and wetting properties of eutectic Sn-Pb, Sn-Zn and Sn-Zn-Bi lead-free solders using wetting balance instrument. *Proceeding of 13<sup>th</sup> Scientific Conference of Electron Microscopy of Malaysia*. 13-15 December 2004. Putrajaya, Malaysia. P. 197-203.
- 1.8 Ramani Mayappan, Ahmad Badri Ismail, Zainal Arifin Ahmad, Luay Bakir Hussain and Tadashi Ariga. (2005) A study on microstructure and the influence of sample perimeter and dipping rate on wetting properties of Sn-Pb and Sn-Zn based lead-free solders. *Proceeding of National Conference on Advances in Mechanical Engineering 2005*. 18-20<sup>th</sup> May 2005. Kuala Lumpur, Malaysia. pp. 265-273.
- 1.9 Ramani Mayappan, Ahmad Badri Ismail, Zainal Arifin Ahmad, Luay Bakir Hussain and Tadashi Ariga. (2005) Joint strength and interfacial microstructure between Sn-Pb, Sn-Zn and Sn-Zn-Bi solders on Cu substrate. *Proceeding of 14<sup>th</sup> Scientific Electron Microscopy Conference 2005*. 5-7<sup>th</sup> December 2005. Penang, Malaysia. P. 1-7.

- 1.10 Ramani Mayappan, Ahmad Badri Ismail, Zainal Arifin Ahmad, Luay Bakir Hussain and Tadashi Ariga. (2006) Effect of fluxes and temperatures on the spreading area of Sn-Zn based lead-free solders. *Proceeding of 3<sup>rd</sup> Post Graduate Research Papers, School of Materials and Minerals Resources Engineering*. March 2006. P. 61-64.
- 1.11 Ramani Mayappan, Ahmad Badri Ismail, Zainal Arifin Ahmad, and Luay Bakir Hussain. (2006) Contact and intermetallic thickness measurement of Sn-Zn based lead-free solders on copper substrates. *Proceeding of International Conference on X-ray and Related Techniques in Research and Industry*. 29-30 November 2006. Putrajaya, Malaysia.



**KAJIAN MENGENAI SIFAT-SIFAT PEMBASAHAN, TINDAKBALAS ANTARAMUKA DAN SIFAT-SIFAT MEKANIKAL PATERI-PATERI Sn-Zn DAN Sn-Zn-Bi KE ATAS PELOGAMAN KUPRUM**

**ABSTRAK**

Secara praktiknya kesemua pemasangan elektronik masa kini menggunakan pateri eutektik Sn-Pb pada antara penyambung. Akibat pertambahan penggunaan peranti elektronik dalam industri serta untuk kegunaan peribadi, maka penggunaan pateri penyambung juga bertambah. Disebabkan oleh masalah keracunan Pb yang berpunca daripada pateri Sn-Pb, Negara-negara di Eropah (WEEE) dan Jepun telah mensasarkan had penggunaan Pb dalam pemasangan elektronik. Hasilnya, diwujudkan peraturan alam sekitar yang menghadkan penggunaan Pb di dalam pateri. Keadaan ini menjadikan satu isu penting untuk mendapatkan pateri yang bebas Pb. Dalam penyelidikan ini logam pateri bebas-plumbum iaitu Sn-9Zn dan Sn-8Zn-3Bi telah diselidik sebagai pengganti berpotensi untuk pateri Sn-40Pb. Satu kajian sistematik telah dilakukan dalam pencirian logam pateri, sifat basahan, tindakbalas antaramuka, sifat-sifat mekanikal dan kinetik penumbuhan logam pateri dengan substrat Cu. Tambahan 3 % berat Bi ke dalam sistem Sn-Zn menurunkan takat lebur sebanyak 3.5°C iaitu hanya 12°C lebih tinggi daripada pateri Sn-40Pb. Pateri ini dapat meningkatkan kebolehasahan pada substrat Cu dengan mengurangkan ketegangan permukaan pateri lebur. Fasa  $\gamma$ -Cu<sub>5</sub>Zn<sub>8</sub> adalah sebatian-antaralogam antaramuka yang utama terbentuk antara pateri Sn-Zn dan substrat Cu dan ketebalan sebatian-antaramuka ini meningkat dengan tempoh dan suhu. Sn-8Zn-3Bi/Cu mempunyai kekuatan sambungan yang lebih tinggi berbanding dengan Sn-9Zn/Cu dan Sn-40Pb/Cu tetapi sambungan pateri ini terdegradasi pada rawatan haba 150°C. Tenaga untuk penumbuhan fasa  $\gamma$ -Cu<sub>5</sub>Zn<sub>8</sub> dalam sistem Sn-9Zn/Cu ialah 44.05 kJ/mol dan untuk sistem Sn-8Zn-3Bi/Cu ialah 55.35 kJ/mol. Tambahan Bi ke dalam sistem Sn-Zn telah membantutkan pertumbuhan fasa  $\gamma$ -Cu<sub>5</sub>Zn<sub>8</sub> dengan menambahkan tenaga untuk pertumbuhan sebatian-antaralogam. Antaramuka di

antara Cu dan pateri Sn-8Zn-3Bi mestilah dihadkan pada suhu bawah 100°C, dan suhu ini memadai untuk penggunaan hampir keseluruhan alat elektronik komersial.

# STUDY ON THE WETTING PROPERTIES, INTERFACIAL REACTIONS AND MECHANICAL PROPERTIES OF Sn-Zn AND Sn-Zn-Bi SOLDERS ON COPPER METALLIZATION

## ABSTRACT

Practically all microelectronic assemblies in use today utilize Sn-Pb eutectic solder for interconnection. Due to the increase in the use of electronic devices within the industry as well as personal use, the usage of solder connections has increased. Emerging environmental regulations worldwide, most notably in Europe (WEEE) and Japan, have targeted the elimination of Pb usage in electronic assemblies, due to the inherent toxicity of Pb. This has made the search for suitable Pb-free solders an important issue for microelectronics assembly. In this research, Sn-9Zn and Sn-8Zn-3Bi lead-free solders were investigated as potential replacements for the Sn-Pb solder. A systematic study was conducted on the solders characteristics, wetting behaviour, the interfacial reaction, mechanical properties and growth kinetics of solders on Cu substrate. The addition of 3wt% of Bi to the Sn-Zn system lowered the melting temperature by 3.5°C which is only 12°C higher than Sn-40Pb solder. It improved the wettability on Cu substrate by reducing the surface tension of the molten solder. The  $\gamma$ -Cu<sub>5</sub>Zn<sub>8</sub> phase is the main interface intermetallic formed between Sn-Zn solders and the Cu substrate and this intermetallic thickness increased with time and temperature. The Sn-8Zn-3Bi/Cu solder joint had higher joint strength than Sn-9Zn/Cu and Sn-40Pb/Cu joints but solder joint degradation occurred at 150°C aging temperature. The activation energy for the growth of  $\gamma$ -Cu<sub>5</sub>Zn<sub>8</sub> phase in Sn-9Zn/Cu and Sn-8Zn-3Bi/Cu systems are 44.05 and 55.36 kJ/mol, respectively. The addition of Bi to the Sn-Zn system had retarded the growth of  $\gamma$ -Cu<sub>5</sub>Zn<sub>8</sub> phase by increasing the activation energy for the intermetallic growth. The direct interface between Cu and Sn-8Zn-3Bi solder should have a temperature limit to be used below 100°C, which is enough for most of the commercial electronics applications.

# CHAPTER 1

## INTRODUCTION

The increase in the use of electronics within industry as well as personal use has been growing exponentially over the past few decades. The driving forces for the microelectronics industry today involve the increasing circuit density at the semiconductor level, global competition in quality, reliability and cost. So, soldering technology has become indispensable for the interconnection and electronic packaging in virtually all electronic devices and circuits.

### 1.1 Problem Statement

Lead-containing solders and especially the eutectic or near-eutectic Sn-Pb alloys have been used extensively in the assembly of modern electronic circuits (Choi et al., 1999; Chen and Lin, 2000; Zeng and Tu, 2002). Many electronic devices, mostly consumer products (i.e. computers, hand phones), are considered disposable because of the introduction of newer, faster technologies each year. Hence, these disposed devices generally end up in landfills.

There is a concern that lead and other elements within the electronic products are considered toxic because there is a potential for leaching from landfills into water sources and becoming a hazard to human health and the surrounding environment (Islam et al., 2006). Even recycling or reclaiming programs are not practical because most circuit boards are too complex to disassemble to reclaim these materials and are not cost effective.

For these reasons, emerging environmental regulations in various countries, most notably in Europe and Japan, have targeted the elimination of lead usage in electronics assemblies (Kim et al., 2005b). Moreover, lead and its compounds have been cited by the Environmental Protection Agency (EPA) as one of the top 17 chemicals posing the greatest threat to human beings and the environment (Abteew and Selvaduray, 2000).

The most aggressive and well-known effort is the European Union's Directive for Waste Electrical and Electronic Equipment (WEEE) proposal, which were initially set to come into effect on 1<sup>st</sup> July 2006. The legislation, which will be regulated by RoHS (Restriction of Hazardous Substances) will limit the disposal of hazardous materials by eliminating certain materials from electrical and electronics products. The WEEE directive was intended to ban the selling, importing and exporting of electrical/electronic containing lead (with some exemption) within the EU countries. The summary of the directive is given in Appendix A.

Subsequently, the Japanese Electronic Industry Development Institute Association (JEIDA) and the Japanese Institute of Electronic Packaging (JIEP) followed the same footsteps to maintain trade with EU countries and marketing edge by promoting "green product" (lead-free) to their customers. Furthermore, many other jurisdictions are planning to put in place similar legislation modeled after EU directives (i.e. China).

Therefore, it is quite an important issue for the electronic industry to develop viable alternative solders (lead-free solders) for electronics assemblies, which can replace the conventional Pb-based solders. The combined effects of these proposals put pressure on the rest of the world to follow suit and generated a large investment in soldering process, equipment and materials development. Many tens of thousands of hours were committed to research and development of lead-free solders during the 1990s. Although the efforts were somewhat uncoordinated, the conclusions of these studies conducted across the globe were remarkably similar: Lead-free soldering was seen to be a technical possibility and indeed, further work has resulted in the commercial availability of lead-free solders and lead-free electronics products (Humpston and Jacobson, 2004).

The threat of legislation has now receded and the European Union has greatly expanded the category of exceptions scheduled for review in 2008 (Puttlitz and Galyon, 2007). Nevertheless, most responsible companies now have accepted a commitment

to clean and “green” manufacturing, whereby no new electronic products may contain lead. It is believed that there will be a progressive transition to lead-free manufacturing for electronics products over the next decade or so, driven largely by companies wishing to promote an environmentally aware image (Humpston and Jacobson, 2004).

A drop-in replacement for the Sn-Pb solder alloy must exhibit various desirable materials characteristic in terms of melting temperature, wettability, electrical and thermal conductivity, thermal expansion coefficient, mechanical strength and ductility, creep resistance, thermal fatigue resistance, corrosion resistance, manufacturability and affordable cost (McCormack and Jin, 1994; Abtey and Selvaduray, 2000; Suganuma, 2001; Zeng and Tu, 2002). Although many Sn-based binary, ternary and quaternary systems are being investigated with improving properties but none of them meet all standards. On the other hand, current processing equipment and conditions (including fluxes) have been optimized for Sn-Pb solder alloys over the last 30 years (Suganuma, 2001).

Many consortiums such as the National Electronic Manufacturing Initiation (NEMI), the National Centre for Manufacturing Sciences (NCMS), IPC and JEIDA are working hard to find a proper Sn-Pb replacement. On top of that, many technical papers, proposing alternative lead-free solders with improved properties were published in recent years.

## **1.2 Lead-free Solder**

Lead in the electronics industry is widely used, so, the push to remove lead from electronics is an extensive and international issue. Seeking to drastically reduce the small amounts of lead found in electronics components, and in most cases totally eliminate it, is thus a huge undertaking for the industry. The efforts require extensive research, evaluation and collaboration not only at the individual company and product sector level, but within the entire electronics industry, to ensure compatibility. Manufacturers are discovering that complying with the rules and converting to lead-free

parts costs millions of dollars. The most efficient solution would be to find a direct substitute (“drop in”) for Sn-Pb solder. Unfortunately, the “drop in” substitute is not available thus far. So, the substitutes for the Sn-Pb solder have been proposed and generally accepted by industry. National Electronic Manufacturing Initiation (NEMI) has recommended Sn-3.9Ag-0.6Cu for reflow soldering and Sn-0.7Cu for wave soldering processes (Zeng and Tu, 2002; Kim et al., 2003a). The Sn-3.9Ag-0.6Cu and Sn-0.7Cu solders have melting temperatures of 217 and 229°C respectively. On contrary, JEIDA recommended Sn-3.0Ag-0.5Cu as an alternative lead free solder and The EU proposed Sn-3.8Ag-0.7Cu as a replacement for conventional Sn-Pb eutectic solder (Kim et al., 2003a).

While these alloys have many merits, there is still scope to replace them with better alloys. These alloys are no “drop-in” replacement for the Sn-37Pb eutectic solder. Furthermore, these alloys have liquidus temperatures 30-50°C higher than Sn-37Pb and, therefore, require significantly higher assembly temperatures than eutectic Sn-37Pb, and are much more expensive. Researchers are working extensively to find other alternatives in Sn-based lead-free solders with small addition of bismuth (Bi) (Yoon et al., 2003), indium (In) (Kim et al., 2005a), silver (Ag) (Kikuchi et al., 2001; Lin and Shih, 2003b), antimony (Sb) (Lee et al., 2005) and aluminium (Al) (Lin and Hsu, 2001). Surprisingly, the toxicity of alloys with low levels of these elements appears not to be an issue (Anonymous, 2005).

### **1.3 Lead-free Solder Used in this Study**

Although there are many lead-free solders available, of these, the Sn-Zn system with some addition of Bi has been expected to be one of the best alternative choices for Sn-Pb replacement. In this study the eutectic Sn-9Zn and Sn-8Zn-3Bi lead-free solders were studied and the near eutectic Sn-40Pb solder was used as reference.

The addition of Bi to Sn-Zn alloy confers several important advantages on them. It lowers the liquidus temperature of the alloy from that of the Sn-9Zn eutectic to a

value that is closer to that of Sn-Pb eutectic solder. So, existing production lines and electronics components do not require major modifications (Yoon et al., 1997; Suganuma et al., 1998; Harris, 1999; Yu et al., 2000a; Suganuma, 2001; Chuang et al., 2002; Choi and Lee, 2002; Wu et al., 2002, Shohji et al., 2004; Kim et al., 2004). It also seems to improve the wetting (Yu et al., 2004) and corrosion performance (Harris, 1999; Kim et al., 2005b). Apart from its favourable melting temperatures, its mechanical properties, e.g. tensile strength, are comparable or better than that of the Sn-Pb solders (Yoon et al., 1997; Wu et al., 2003; Hirose et al., 2004; Kim et al., 2005b). It is also anticipated that the addition of Bi to the Sn-Zn system will have a beneficial effect on the intermetallic formation and subsequently to the growth rate of intermetallic compounds (Islam et al., 2005a).

Although Bi is recognized as a rare metal and information on the earth's total resource amount and its annual production amount is still ambiguous, it is estimated that the Bi supply is enough for solders even with Sn-58Bi eutectic solder system (Suganuma, 2001). So, compared with other rare metals, Bi is readily available if it is used as soldering material.

The microelectronics industry is extremely cost conscious. The history of the industry has been to continuously produce higher performance at lower cost (Abtew and Selvaduray, 2000). Since cost of the product is the resultant of the cumulative cost of the components, the cost of lead-free solder alloys can impact the cost of the finished product. So, cost is another important factor in the adoption of solders for practical applications. In general, taking cost of raw metals into consideration, most lead-free solders cost about two to three times more than Sn-Pb solders (Suganuma, 2001). The cost of Zn and Bi is generally cheaper than other raw metals like Ag and In (Abtew and Selvaduray, 2000; Kim et al., 2005b). So, the Sn-9Zn and Sn-8Zn-3Bi solders are a potential system for replacing Sn-Pb eutectic alloy from the cost point of view.



There are several lead-free solders, which are patented. Among them are Sn-20In-2.8Ag, Sn-2.5Ag-0.8Cu-0.5Sb (Castin™), Sn-2Cu-0.8Sb-0.1Ag and Sn-3.4Ag-4.8Bi. This implies that the number of suppliers could be restricted. Patented lead-free solder may require licensing or royalty agreements before use. The prospect of an entire industry being dependent on one supplier for its solder alloys is not desirable. If this were to happen, the likelihood of future price decreases would be extremely small as there will be no competition. So, from an availability standpoint, an unpatented solder alloy, with multiple and stable price structure and no geopolitical concerns, would be most desirable. Being an unpatented solder, the Sn-9Zn and Sn-8Zn-3Bi solders is a possible replacement from this point of view.

#### **1.4 Importance of Study**

Although lead-free solders lack of the toxicity problems, however, the recently employed lead-free solders do not have a long history and well-established manufacturing and engineering database. Consequently, the inertia for acceptance of lead-free solders by design engineers and manufacturers will remain pending thorough examinations of these materials. However, research studies in recent years by organizations and researchers, characterizing various properties and performance of lead-free solders have alleviated some of the reluctance for acceptance (Plumbridge, 1996). For the need of lead-free solder in practical usage, scientific information is needed that enables us to understand the various phenomena occurring in electronics that employ lead-free solders. The development of a lead-free solder alloy that has all the desirable properties will be a formidable task unless a scientific basis has been established.

The reliability of soldered devices is related to wettability of the solder to the substrate and to microstructural evaluation of the joint during soldering operation or in use (Yoon et al., 1997). It is believed that the interface reaction products between solder alloys and substrate have a great effect on mechanical properties of the

solder/substrate joints. In addition, the formation of intermetallic compounds at the interface during soldering processes plays an important role in wettability of the solder. Accordingly, the reliability of solder joints will be strongly affected by the type and extent of the reaction between solder and substrate (Vianco et al., 1995; Lee et al., 1998; Choi et al., 1999). As such, solder-substrate interactions are increasingly important and need deeper understanding. Furthermore, with the inevitable use of lead-free solder alloys, research on the formation of the intermetallic layer in lead-free solders have become more important than that with Sn-Pb solders (Yu et al., 2005).

Although the Sn-9Zn and Sn-8Zn-3Bi lead-free solders were studied by many researchers (Suganuma et al., 1998; Suganuma et al., 2000; Kim et al., 2003b; Shohji et al., 2004; Islam et al., 2005a; Kim et al., 2005b, Islam et al., 2006), there is still a general lack of engineering information about these solders with respect to their interaction with copper (Cu) substrate. Suganuma et al. (1998) reported the wetting, interface microstructure and tensile strength of Sn-9Zn solder on Cu substrate after soldering at 290°C without any aging. A similar study was conducted by Suganuma et al. (2000) by using Sn-9Zn solder paste. Suganuma et al. (2000) study the 150°C aging effect on solder joint degradation. The thermal and mechanical properties of the bulk Sn-9Zn and Sn-8Zn-3Bi solders were conducted by Kim et al. (2003b) by investigating the microstructural changes under different cooling rate. The creep properties of the bulk Sn-8Zn-3Bi solder were studied by Shohji et al. (2004) at different temperatures. The interfacial reaction between Sn-9Zn and Sn-8Zn-3Bi solders and Cu substrate were studied by Islam et al. (2005a) using reflow method. The reflow was done at 230°C for duration of 20 minutes. A similar reflow method was used by Kim et al. (2005b) to study the intermetallic growth between Sn-8Zn-3Bi solder and Cu substrate. Kim et al. (2005b) selected the aging temperatures between 70 and 150°C for duration of 100 days. Islam et al. (2006) conducted microhardness test on bulk Sn-9Zn and Sn-8Zn-3Bi solders and wetting (spreading) on Cu substrate at 230 and 250°C.

In the present study, the wetting characteristic (spreading and dipping) of the Sn-9Zn and Sn-8Zn-3Bi bulk solders were investigated. The as-soldered interface formed with Cu substrate after soldering for 1 minute was studied. Solder joints were fabricated by soldering at 240°C and the joint strength (butt-joint and single lap joint) and phase transformation studies were conducted at different crosshead speed and aging. The intermetallic growth study was conducted for aging temperatures between 50 to 150°C for duration of 700 hours by using the single lap joint specimens.

There can be a number of intermetallic compounds formed at the substrate and solder interface during soldering. However, only the intermetallic compounds that form first during the soldering process have a significant effect on wetting. So, the wetting properties and intermetallic formation of the solders' performance with respect to different fluxes and temperatures need to be explored.

During storage or in use, the intermetallics generated during soldering grow further in thickness or increase in number, especially if the operational temperatures are well above the ambient (Laurila et al., 2005). Generally, the main cause of breakdown in solder joints is known to be the excessive growth of brittle intermetallic compound because it bonds mechanically with the solder and substrate. This in turn, degrades the interfacial strength and the mismatch in physical properties such as thermal expansion coefficient and the elastic modulus (Hwang et al., 2003). In this way, the growth behavior of the intermetallic and the mechanical properties of the solder joints significantly affect the performance and reliability of the joints (Frear, 1996; Yoon et al., 1999; Yu et al., 2005). Therefore, the interaction between solder/substrate needs to be investigated more systematically from the soldering stage to the servicing stage to have a better understanding of the reliability of soldered joints. Furthermore, the knowledge on the reliability of the solders with regards to phase transformation, mechanical properties and growth kinetics during long-time aging is also generally lacking.

## **1.5 Objective of the Study**

The primary objectives of this work are:

- (1) Study the wetting characteristics of Sn-40Pb, Sn-9Zn and Sn-8Zn-3Bi solders by spreading and dipping methods on copper metallization. The effect of flux chemistry or type and temperature on wetting characteristics is also investigated.
- (2) To investigate the intermetallic formed between solders and Cu substrate and study their growth kinetics.
- (3) To determine the tensile property (butt-joint) on the as-soldered joint at different crosshead speeds.
- (4) To study the effect of aging on phase transformation and mechanical properties of solder joint using single lap shear test.

## **1.6 Structure of the Thesis**

In this thesis the background theory and the relevant literature survey are presented in the second chapter. This is followed, in chapter three, by a description of all of the methods and techniques used in experiment, characterization and test procedures. Chapter four consists of the details of the results and discussions. Chapter five presents the conclusions of this thesis and suggesting future works.

## **CHAPTER 2 LITERATURE REVIEW**

### **2.1 Soldering**

The American Welding Society defines soldering as a joining process wherein a coalescence between metal parts is produced by heating to temperatures below 425°C using filler metals (solders) having melting temperatures below those of the base metal (Frear et al., 1994). Manko (2001) defines soldering as a metallurgical joining method using a filler metal (the solder) with a melting point below 315°C and to achieve this, wetting is needed for the bond formation and requires neither diffusion nor intermetallic compound growth with base metal. Metallurgical bonds are connections between metals only. These are the bonds in which metallic continuity from one metal to the other is established.

### **2.2 Lead**

Lead is a heavy metal found naturally in the earth that has been used in many ways for hundreds of years. Lead was added to gasoline from the 1920s until it was phased out, beginning in the 1970s. Until the 1970s, lead was added to paint used in homes and for another decade it was used in solder to seal food cans and connect plumbing pipes. Lead consumption in industries is listed in Table 2.1. Battery manufacturing accounts the vast majority of the lead consumed and electronic industries consumes less than 0.5% each year. On the other hand, lead recycling in battery industry is almost 100% effective. However, virtually none of the 66 000 tons lead used by the electronic and lighting industries is recycled (Humpston and Jacobson, 2004). Because lead does not decompose or deteriorate, it does not go away but remains in homes, in the soil alongside roadways and in some water pipes. The waste in landfill sites is subjected to chemical attack by rain water, from where leached-out constituents, including lead, eventually find their way into drinking water supplies.

Table 2.1: Major uses of lead globally (Anonymous, 2004a)

Product	Consumption (%)
Storage Batteries	80.8
Paint, Ceramics, Chemicals, Pigments	4.8
Ammunition	4.7
Other uses	9.2
Electronic Solder	<0.5

### 2.3 Sn-Pb Solder and Electronics Industries

Sn-Pb solders for metal interconnections have a long history, dating back 2000 years. This solder and the alloys developed with it have long provided and continue to provide many benefits, such as ease of handling, low melting temperatures, good workability, ductility and excellent wetting on Cu and its alloys (Suganuma, 2001). Furthermore, the eutectic Sn-Pb solder provides excellent electrical conductivity and suitable mechanical strength (Cheng and Lin, 2002). It is also a critical material in virtually all electronics because it is uniquely capable of meeting high technology performance requirements in a cost efficient manner.

### 2.4 Pb-free Solders Requirements

When trying to identify an alternative to the Sn-Pb solders, it is important to ensure that the properties of the replacement solder are comparable to or superior than Sn-Pb solders. There are strict performance requirements for solder alloys used in microelectronics (Abtew and Selvaduray, 2000). In general, the solder alloy must meet the expected levels of electrical and mechanical performance, and must also have the desired melting temperature. It must adequately wet common printed circuit board (PCB), form inspectable solder joints, allow high volume soldering and rework of defective joints, provide reliable solder joints under service conditions and must not

significantly increase assembly cost. The major performance characteristics of the solder are listed below:

- (i) Non-toxic
- (ii) Acceptable melting and processing temperature: One of the most sensitive parameters for the quality of soldered joints is soldering temperature. The melting temperature of Sn-Pb eutectic alloy is 183°C, and the typical soldering temperatures are 230 and 250°C for reflow and wave soldering, respectively. The temperature margin beyond the melting temperature of solder is 50°C for reflow (Suganuma, 2001). The melting point of a solder should be low enough to avoid thermal damage to the assembly being soldered and high enough for the solder joint to bear the operating temperatures.
- (iii) Narrow Paste Range: The pasty range is the temperature range between solidus and liquidus, where alloy is part solid and part liquid. When the pasty range is narrow, the solder needs shorter time to solidify. The criteria set by NIST (National Institute of Standards and Technology) (Anonymous, 2004b), the acceptance level is <30°C.
- (iv) Good Solder Wetting: The bond between the solder and the base metal is formed only when the solder wets the base metal properly. A high Sn content ensures this and thus forms a strong bond (Wu et al., 2004).
- (v) Available and Affordable: There should be adequate supplies or reserves of candidate metals. Some potentially viable compounds may not be available in sufficient quantity to satisfy worldwide demand should the material is chosen. The world reserves for some of the solder candidate metal are listed in Table 2.2.
- (vi) Form Reliable Joint: Reliability of a solder alloy is mainly dependent on the coefficient of thermal expansion, elastic modulus, yield strength, shear strength, fatigue and creep behaviour of the alloy.

Table 2.2: World reserves for raw metals (Anonymous, 2004a)

Raw Metals	World Reserves (Thousand Metric Tons)
Lead (Pb)	140,000
Zinc (Zn)	440,000
Copper (Cu)	650,000
Antimony (Sb)	3200
Bismuth (Bi)	260
Tin (Sn)	12000
Silver(Ag)	420
Indium (In)	6

(vii) Cost: Manufactures of electronics systems are likely to change to an alternative solder with an increase cost unless it has demonstrated better properties or there is legislative pressure to do so (Wu et al., 2004). The unit cost of the major elemental metals used in solders is summarized in Table 2.3. In Table 2.4, the cost of some solder alloys is listed. On an elemental basis, Pb and Zn are the cheapest metals and Ag and In falls in a very expensive category. All of the Pb-free solder alloys are more expensive than the eutectic Sn-Pb alloy, which costs US5.87/kg. Some of the alloys are in the US7.70–8.80/kg range, other alloys cost between US11.00 and 16.50/kg. The Sn–In–Ag ternary alloy costs the highest of US51.63/kg because the high cost of Ag and In. If cost were the sole deciding factor, it is highly unlikely that the electronics industry would adopt an alternative solder. There has to be a demonstrated benefit in using one or more of the Pb-free solder alloys. For example, a significant improvement in reliability that can offset the cost increase could justify the adoption of a higher cost alternative (Abtew and Selvaduray, 2000). However, in the case of Pb-free solders, the driving force is government legislation, which would eventually prohibit the use of Sn-Pb solder, which happens to have a long track record. While price fluctuations of minor components have minimal effect on the alloy cost, but price fluctuations of major constituents can be expected to have a more significant effect, thus



making In a less attractive choice. The price of the patented solders, Castin™, increases from US2.21/kg in 1997 to US12.06/kg in 1999.

Table 2.3: Raw metals cost

Element	Cost (US/kg) (2 January 1997) (Abtew and Selvaduray, 2000)	Cost (US/kg) (2 March 1999) (Anonymous, 2004b)
Lead (Pb)	1.10	0.99
Zinc (Zn)	1.08	1.10
Copper (Cu)	2.24	1.43
Antimony (Sb)	2.64	1.76
Bismuth (Bi)	7.15	7.48
Tin (Sn)	8.67	7.70
Silver (Ag)	153.19	185.24
Indium (In)	194.59	275.00

Table 2.4: Solder alloys cost

Alloy	Cost (US\$/kg) (12 January 1997) (Abtew and Selvaduray, 2000)	Cost (US\$/kg) (2 March 1999) (Anonymous, 2004b)
Sn-37Pb	5.87	-
Sn-58 Bi	7.79	7.57
Sn-20In-2.8Ag	51.63	66.13
Sn-10Bi-5Zn	8.14	-
Sn-9Zn	7.99	7.11
Sn-7.5Bi-2Ag-0.5Cu	11.42	-
Sn-3.2Ag-0.5Cu	13.27	-
Sn-3.5Ag-1.5In	16.52	17.93
Sn-2.5Ag-0.8Cu-0.5Sb (Castin™)	2.21	12.06
Sn-3.5Ag	13.73	13.90
Sn-2Ag	11.55	-
Sn-0.7Cu	8.62	7.66
Sn-2Cu-0.8Sb-0.1Ag	8.78	-
Sn-5Sb	8.36	7.41
Sn-4Ag-0.5Cu	-	14.41
Sn-3.4Ag-4.8Bi	-	13.73
Sn-3.5Ag-3Bi	-	13.02

The current processing equipment and conditions for electronics assembly were optimized for Sn-Pb solders. Any new conditions for lead-free alloys must ensure both productivity and reliability at least equivalent to the present level of Sn-Pb solders. In contrast, melting temperatures for some typical lead-free solder are higher than Sn-

Pb eutectic solder, which makes the process window narrower. Because some of the electronic components (such as capacitors and connectors) cannot at present withstand an increase in reflow temperature, we need to modify or develop processing conditions to incorporate heat-resistant components (Suganuma, 2001). In wave soldering, the soldering temperature does not need increasing, while wetting of most lead-free solders on substrate needs to be improved by modifying fluxes and designing new approaches.

## **2.5 The Development of Pb-free Solders**

A brief description of Sn-based major binary, ternary and quaternary systems is provided in this section. A relatively large number of Pb-free solder alloys have been proposed, and are summarized in Table 2.5 with their elemental compositions and melting temperatures. The melting temperatures are presented in the solidus,  $T_s$ , liquidus,  $T_l$ , and eutectic temperatures,  $T_e$ . The solder alloys are binary, ternary and some are even quaternary alloys. Since the properties of the binary Pb-free solders cannot fully meet the requirements for applications in electronic packaging, additional alloying elements were added to improve the performance of these alloys (Wu et al., 2004). Temperatures for ternary and quaternary systems were frequently reported in the literature as 'melting temperature',  $T_m$ , and therefore are listed as such in Table 2.5 as well. It can be noticed that most of the alloys are Sn-based. The main alloying elements are Zn, In, Bi, Ag, Sb and Cu. Rare earth elements such as cesium (Cs) and lanthanum (La) were added to some Sn-Zn binary alloys to overcome the oxidation problem.

For binary and higher systems, a unique 'melting temperature' can be expected only for eutectic compositions or for compositions that melt congruently. Other compositions (off-eutectic) can be expected to melt over a range of temperatures, with melting begins at the solidus temperature and completes at the liquidus temperature.

Table 2.5: Proposed lead-free solder alloys with their melting temperature ( $T_m$  = Melting Temperature,  $T_s$  = Solidus Temperature,  $T_l$  = Liquidus Temperature,  $T_e$  = Eutectic Temperature)

Alloy Composition (wt%)	$T_m$ (°C)	$T_s$ (°C)	$T_l$ (°C)	$T_e$ (°C)	Reference
Sn-37Pb				183	Abtew and Selvaduray, 2000
Sn40Pb		183	187		Abtew and Selvaduray, 2000
Sn-2Ag		221	225		Abtew and Selvaduray, 2000
Sn-50In		117	125		Cheng and Lin, 2002
Sn-3Cu		227	275		Abtew and Selvaduray, 2000
Sn-4Ag		221	225		Abtew and Selvaduray, 2000
Sn-42Bi		139		170	Abtew and Selvaduray, 2000
Sn-42In		117	140		Abtew and Selvaduray, 2000
Sn-36In		117	165		Abtew and Selvaduray, 2000
Sn-5Sb		234	240		Abtew and Selvaduray, 2000
Sn-0.7Cu				227	Wu et al., 2004
Sn-3.5Ag (eutectic)				221	Wu et al., 2004
Sn-58Bi				138	Cheng and Lin, 2002
Sn-3.5Ag-1Zn	217				Abtew and Selvaduray, 2000
Sn-3.6Ag-1.5Cu	225				Abtew and Selvaduray, 2000
Sn-4Ag-7Sb			230		Abtew and Selvaduray, 2000
Sn-4Ag-0.5Cu	218				Anonymous, 2004b
Sn-3.4Ag-4.8Bi <sup>TM</sup>		208	215		Anonymous, 2004b
Sn-3.5Ag-3Bi		216	220		Anonymous, 2004b
Sn-2.8Ag-20In <sup>TM</sup>		179	189		Anonymous, 2004b
Sn-4Sb-8Zn		198	204		Abtew and Selvaduray, 2000
Sn-9Zn-10In	178				Abtew and Selvaduray, 2000
Sn-6Zn-6Bi	127				Abtew and Selvaduray, 2000
Sn-4.7Ag-1.7Cu	217				Abtew and Selvaduray, 2000
Sn-4Cu-0.5Ag		216	222		Abtew and Selvaduray, 2000
Sn-2Ag-6Zn-0.8Cu		217	217		Abtew and Selvaduray, 2000
Sn-8Zn-10In-2Bi	175				Abtew and Selvaduray, 2000
Sn-2.5Ag-0.8Cu-0.5Sb <sup>TM</sup>		213	219		Anonymous, 2004b
Sn-2Ag-0.8Cu-8Zn		215	215		Abtew and Selvaduray, 2000
Sn-Zn-RE					Wu et al., 2002
Sn-2.8Ag-0.5Cu				218	Rizvi et al., 2006
Sn-2.8Ag-0.5Cu-1.0Bi				214	Rizvi et al., 2006
Sn-9Zn-1.5Ag-0.5Bi		195.9	200.9		Liu et al., 2004
Sn-9Zn-0.5Ag	199.2				Chen et al., 2006
Sn-9Zn-0.4Ag	198.3				Chen et al., 2006
Sn-9Zn-0.5Ga	196.1				Chen et al., 2006

As can be seen from Table 2.5 the vast majority of the Pb-free solder alloys have melting points or liquidus temperatures in the low 200°C range, though there are a few alloys with significantly lower melting temperatures, primarily among the Bi and In systems. The Sn–Cu systems have liquidus temperatures that are significantly higher than the 183°C eutectic temperature of the Sn-Pb system. Too high a liquidus or melting temperature means that processing temperatures have to be higher.

## 2.6 Phase Diagrams

Knowledge of phase equilibrium of solder/alloy and solder/substrate systems provides the basic roadmap for the initial selection of candidate solders and contributes

to the understanding of solder wetting and spreading. Phase diagrams data provide not only information about the liquidus and solidus temperatures of a candidate solder alloy, but also information about possible intermetallic phase formation, either within the solder during solidification or in reaction with the substrate material by combination of isothermal solidification and solid-state reaction.

Most binary phase diagrams that are of interest are fairly simple and most of the phase boundaries are well established. Since the binary Sn-based system are key system for the evaluation of candidate solder alloys, important features of these systems will be briefly discussed.

### **2.6.1 Sn-Pb Phase Diagram**

The phase diagram of Sn-Pb binary system is shown in Fig. 2.1. The phase diagram of this system is well established and a number of thermodynamic assessments are available for this system. The Sn-Pb phase diagram is characterized by two solid phases each with substantial solid solubility and a liquid phase. Further, the system is characterized by a simple eutectic with a significant depression of the liquidus temperature by almost 50°C, from pure Sn at 232°C to the binary eutectic (Sn-37Pb) at 183°C (Suganuma, 2004). The microstructure on solidification is a mixture of Sn and Pb solid solutions. The solid solubility of Sn in Pb at 183°C is about 19 wt.% Sn, which decreases to  $1.3 \pm 0.5$  wt.% at room temperature (Gurusamy, 2000).

### **2.6.2 Sn-Zn Phase Diagram**

Fig. 2.2 shows the Sn-Zn binary phase diagram, which has a eutectic point at 198.5°C and composition of 91.1Sn-8.9Zn (wt.%). At this temperature, the liquid decomposes into the two terminal solid solutions. Its microstructure consists of two phases: a body-centered tetragonal Sn matrix phase and a secondary phase of hexagonal Zn containing less than 1 wt.% Sn in solid solution. The solid solubility of Sn in Zn is less than 0.05 wt.% and the maximum solid solubility of Zn in Sn has been

estimated as being ~2 wt.% (Abtew and Selvaduray, 2000). The microstructure of the eutectic Sn-9Zn can be expected to be lamellar, consisting of alternating Sn-rich and Zn-rich phases.

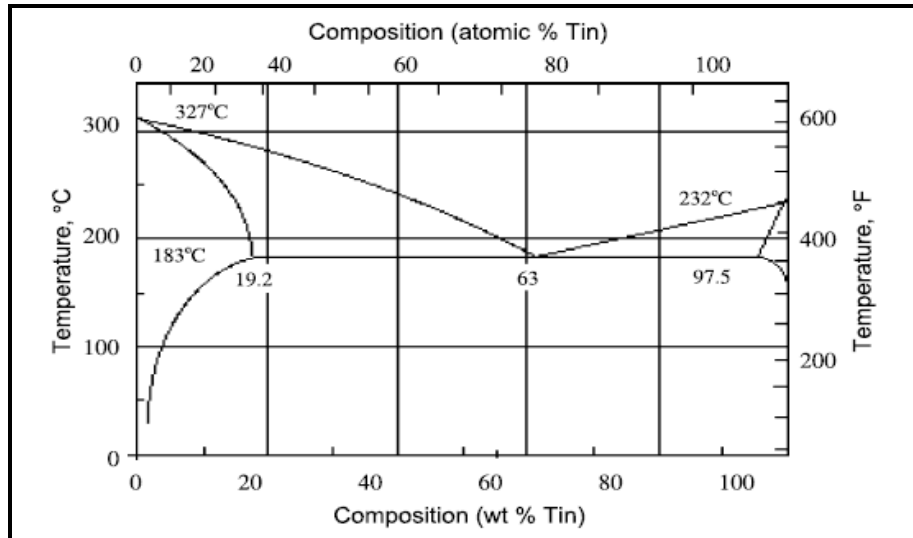


Fig. 2.1: Sn-Pb binary phase diagram (Humpston and Jacobson, 2004)

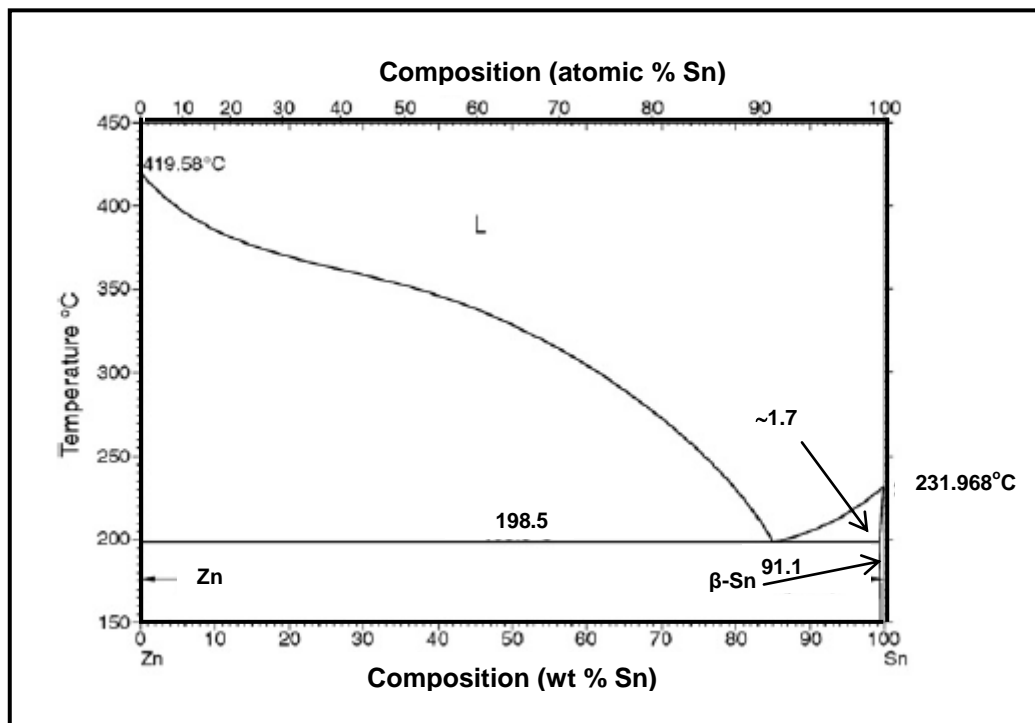


Fig. 2.2: Sn-Zn binary phase diagram (Massalski, 1992)

### 2.6.3 Sn-Cu Phase Diagram

Fig. 2.3 shows the phase diagram of Sn-Cu system. In addition to liquid and the two terminal solution phases, (Cu) and (Sn), this system has seven intermediate phases,  $\beta$ ,  $\gamma$ ,  $\text{Cu}_{41}\text{Sn}_{11}$  ( $\delta$ ),  $\text{Cu}_{10}\text{Sn}_3$  ( $\zeta$ ),  $\epsilon\text{-Cu}_3\text{Sn}$ ,  $\eta\text{-Cu}_6\text{Sn}_5$  and  $\eta'\text{-Cu}_6\text{Sn}_5$  ( $\eta$  and  $\eta'$  is the high and low-temperature forms) (Kattner, 2002). All of the intermediate phases form by peritectic or peritectoid reactions. All of the Cu-rich intermediate phases decompose in eutectoid reactions at temperatures above 350°C and therefore, only the  $\epsilon\text{-Cu}_3\text{Sn}$ ,  $\eta\text{-Cu}_6\text{Sn}_5$  and  $\eta'\text{-Cu}_6\text{Sn}_5$  phases are of interest for solder applications.

The  $\epsilon\text{-Cu}_3\text{Sn}$  and  $\eta\text{-Cu}_6\text{Sn}_5$  intermetallic phases are stable at temperatures below 300°C. The  $\epsilon$  phase has a composition range between 37.9 and 38.5 wt.% (24.5-25.9 at.%) Sn, and corresponds very closely to the composition  $\text{Cu}_3\text{Sn}$ . The  $\eta$  phase has Sn concentration of between 60.0 and 61.0 wt.% (43.5-44.5 at.%), and corresponds to the composition  $\text{Cu}_6\text{Sn}_5$  (Massalski, 1992).

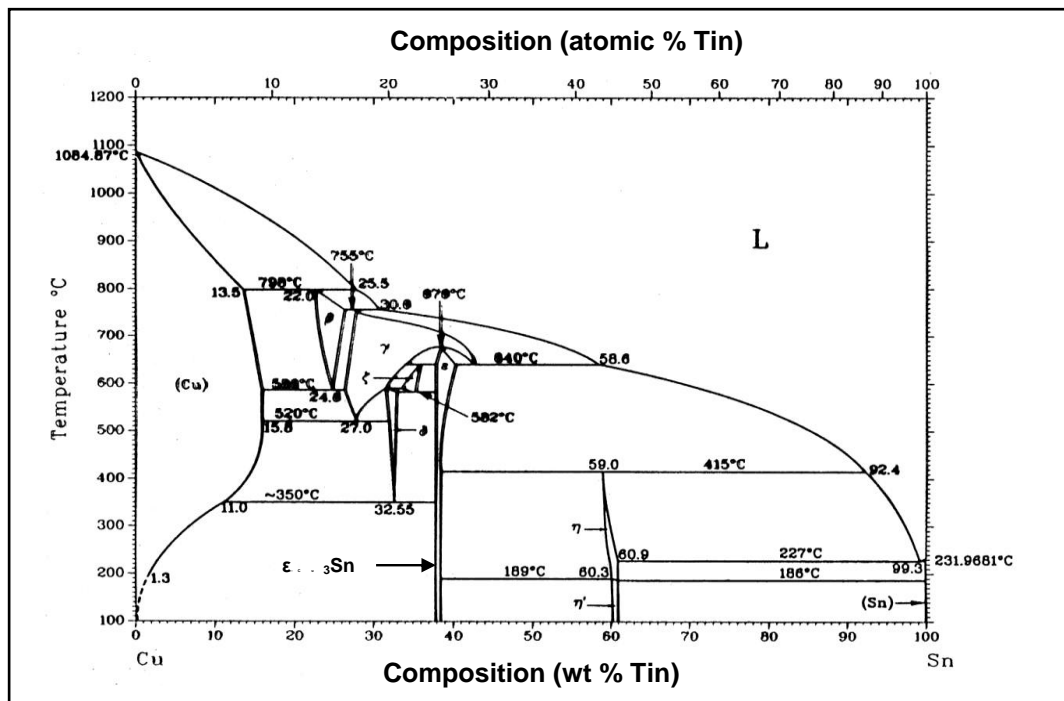


Fig. 2.3: Cu-Sn binary phase diagram (Massalski, 1992)

## 2.6.4 Cu-Zn Phase Diagram

The Cu–Zn system forms three intermediate phases with relatively broad ranges of stoichiometric as shown in Fig. 2.4. The  $\gamma$ -Cu-Zn phase is known to have a solubility range of 57.5-71.5 wt.% (57-70 at%) Zn and  $\text{Cu}_5\text{Zn}_8$  type structure (Massalski, 1992). The  $\beta$  and  $\epsilon$  intermediate phases also exist in addition to two terminal solid phases and  $\epsilon$  phase has a solubility range of 79.0-88.0 wt.% (78-88 at%) Zn and a hcp structure (Lee et al., 1998; Massalski, 1992).

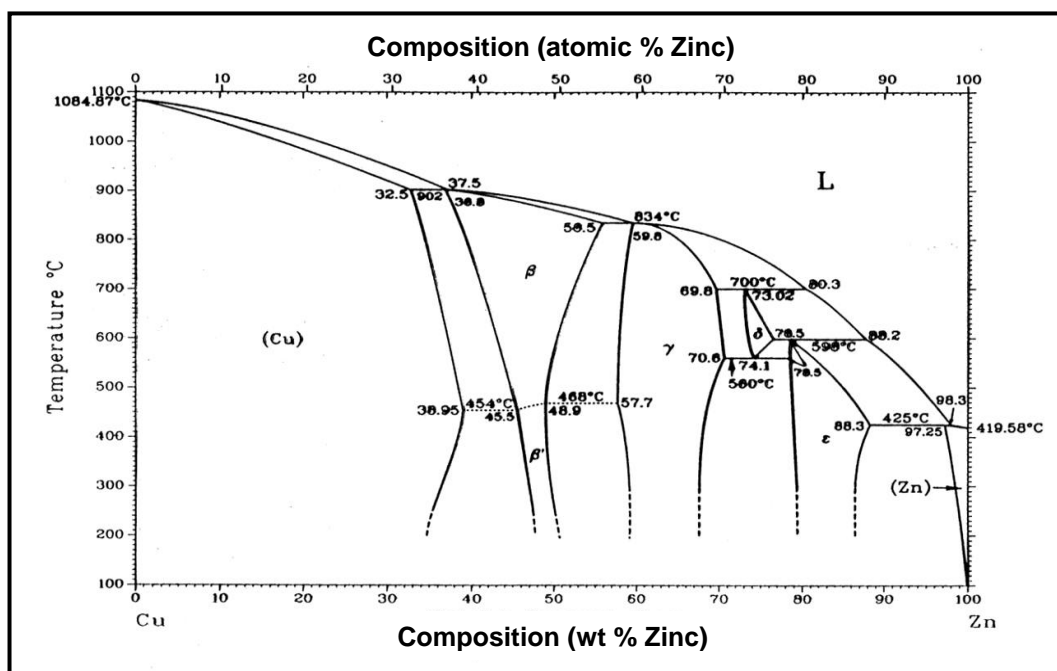


Fig. 2.4: Cu-Zn binary phase diagram (Massalski, 1992)

## 2.6.5 Sn-Bi Phase Diagram

The Sn-Bi phase is shown in Fig. 2.5. The solubility of Bi in Sn at eutectic temperature is nearly 20 wt.%. When the temperature is below the eutectic point, small Bi-rich particles form within the Sn-rich phase (Frear et al., 1994). This precipitation is due to the fact that the solubility of Bi in Sn decreases significantly as the temperature is lowered below the eutectic point. At room temperature, the solubility of Sn in Bi probably less than 1 wt.% (Barry and Thwaites, 1983; Zhao et al., 2004).

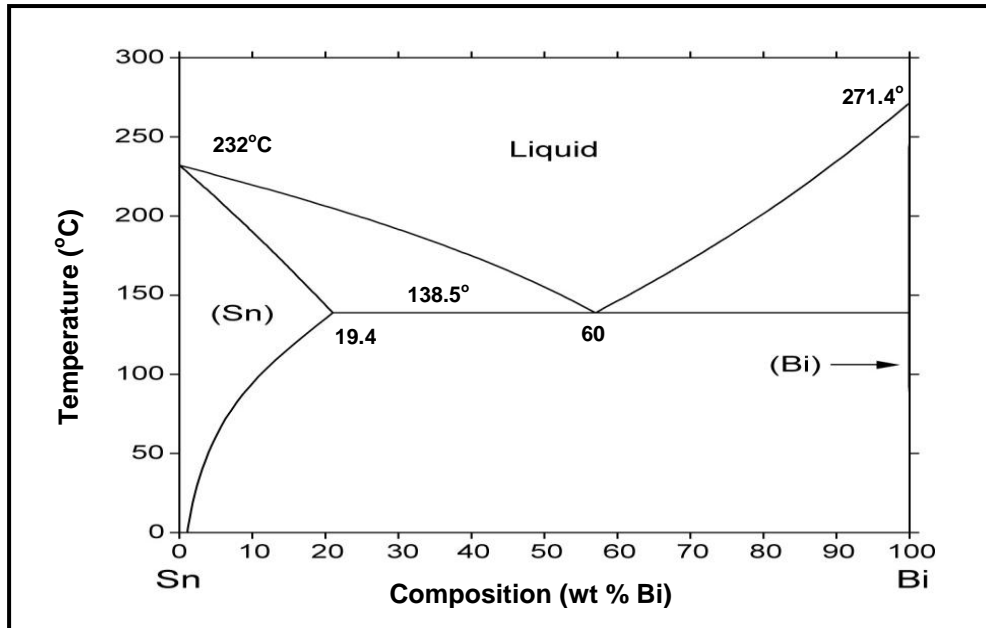


Fig. 2.5: Sn-Bi binary phase diagram (Barry and Thwaites, 1983)

### 2.6.6 Bi-Zn Phase Diagram

Fig. 2.6 shows the phase diagram of Bi-Zn system. This system exhibits eutectic at 2.7 wt.% Zn at 254.5°C. Since Bi does not react with Zn, no intermetallic formation is expected.

### 2.6.7 Cu-Pb Phase Diagram

Fig 2.7 shows Cu-Pb phase diagram and the two metals are virtually immiscible in each other and no intermetallic formed between them. The eutectic reaction in this system occurs on the lead side at 326°C at eutectic composition of 0.0006 wt.% Cu. At room temperature, the solubility limit of Cu is < 0.007 wt.% Cu (Gurusamy, 2000).



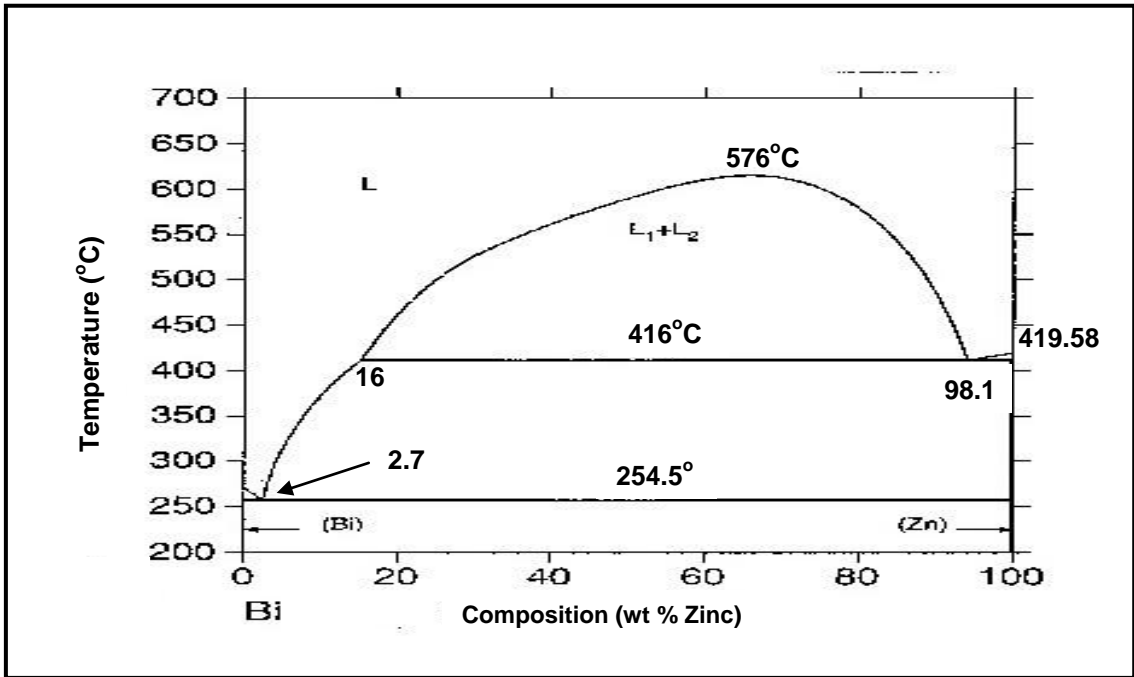


Fig. 2.6: Bi-Zn binary phase diagram (Massalski, 1992)

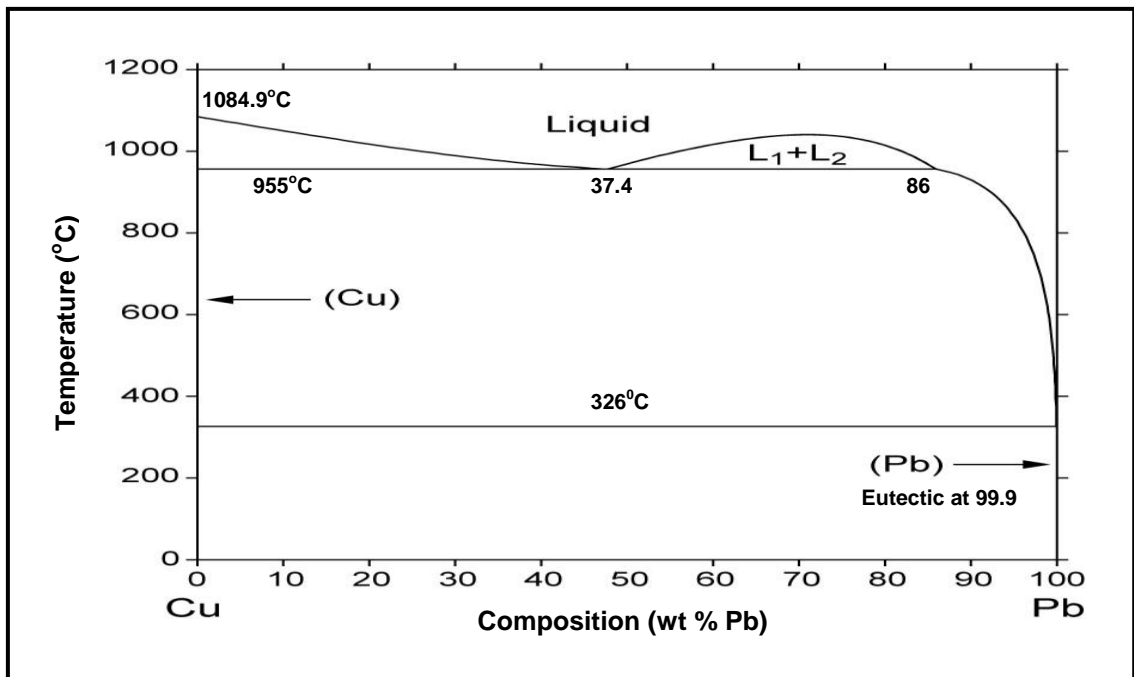


Fig. 2.7: Cu-Pb binary phase diagram (Blaskett and Boxall, 1990)

### 2.6.8 Bi-Cu Phase Diagram

The Bi-Cu phase diagram is shown in Fig. 2.8. The system exhibits eutectic behaviour with a eutectic composition of 99.8 wt% Bi, and a eutectic temperature of 270.6°C. Bi does not form intermetallic compounds with Cu.

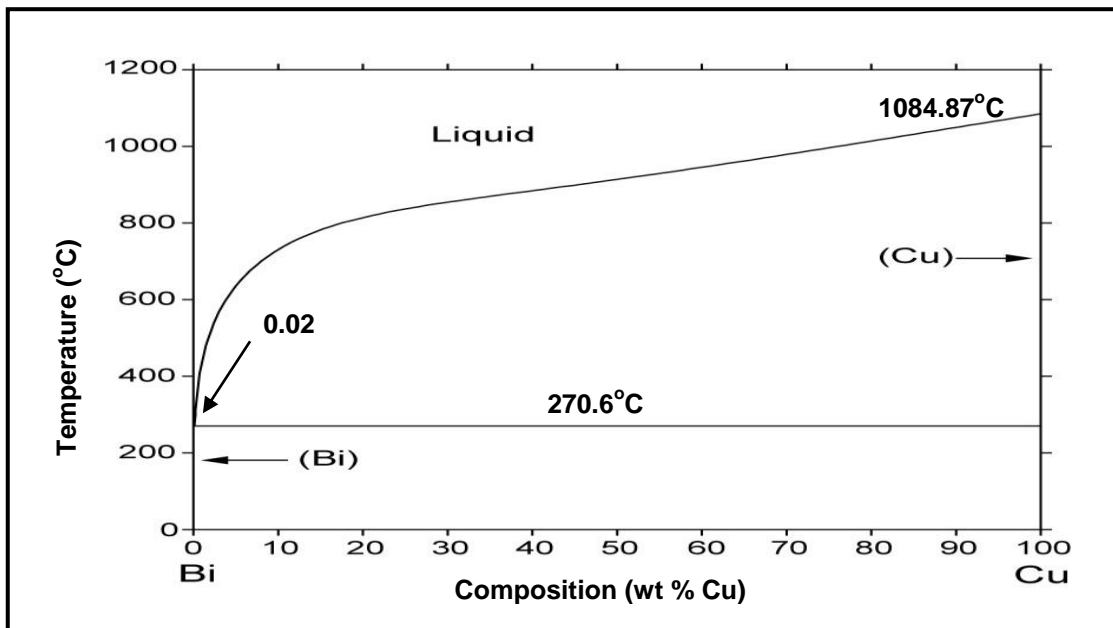
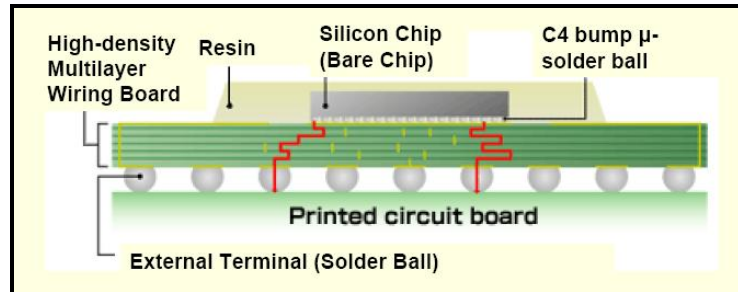


Fig. 2.8: Bi-Cu binary phase diagram (Massalski, 1992)

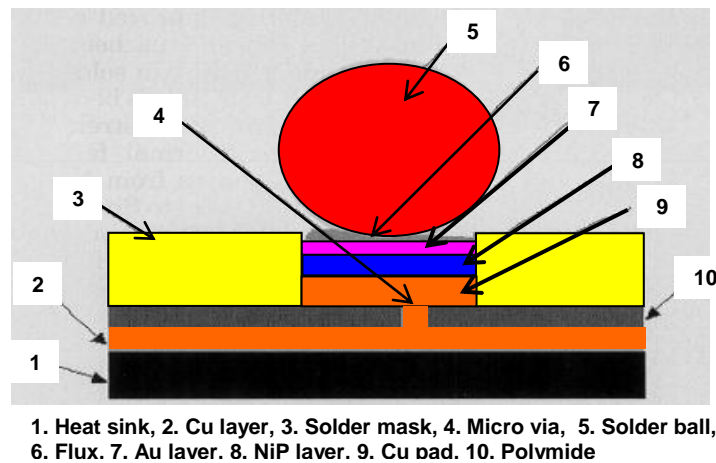
### 2.7 Solder Ball and Copper as Interconnect Material

As a joining material, solder provides electrical, thermal and mechanical continuity in electronics assemblies (Abtey and Selvaduray, 2000). The performance and quality of the solder are crucial to the integrity of a solder joint, which in turn is vital to the overall functioning of the assembly. Solders are used in different levels of the electronic assembly sequence, shown in Fig. 2.9(a). As a die bonding material, the solder provides the electrical and mechanical connection between the silicon die and the bonding pad. It also serves as path for heat dissipation of the heat generated by the semiconductor. Bonding of the die to a substrate and its encapsulation is referred to as Level 1 packaging. The next level of assembly and interconnect, referred as Level 2

packaging, is where the component (encapsulated silicon die) is mounted on a printed circuit board using solder balls (Fig 2.9(a)).



(a)



(b)

Fig. 2.9: Cross section of the package: (a) Level 1 and Level 2 interconnection (b) A schematic illustration of Cu position in interconnection (Islam and Chan, 2005)

Although the Al alloy has performed well as an interconnect conductor for a long time, the trend of miniaturization has recently demanded a change due to the following reasons (Tu, 2003):

- (i) the resistance-capacitance (RC) delay in signal transmission in fine lines,
- (ii) the concern of electromigration. For the use of narrower and narrower lines, not only the line resistance increases, but also the capacitance between lines will drag down signal propagation.